0026-895X/07/7105-1329–1340$20.00
MOLECULAR PHARMACOLOGY
Copyright © 2007 The American Society for Pharmacology and Experimental Therapeutics
Mol Pharmacol 71:1329–1340, 2007

Vol. 71, No. 5
30304/3196647
Printed in U.S.A.

Real-Time Analysis of Agonist-Induced Activation of Protease-Activated Receptor 1/Gα_{i1} Protein Complex Measured by Bioluminescence Resonance Energy Transfer in Living Cells

Mohammed A. Ayoub, Damien Maurel, Virginie Binet, Michel Fink, Laurent Prézeau, Hervé Ansanay, and Jean-Philippe Pin

Centre National de la Recherche Scientifique, Unité Mixte de Recherche 5203, Montpellier, France (M.A.A., D.M., V.B., L.P., J.P.P.); Institut National de la Santé et de la Recherche Médicale U661, Montpellier, France (M.A.A., D.M., V.B., L.P., J.P.P.); Université de Montpellier 1, Montpellier, France (M.A.A., D.M., V.B., L.P., J.P.P.); Université de Montpellier 2, Montpellier, France (M.A.A., D.M., V.B., L.P., J.P.P.); Institut de Génomique Fonctionnelle, Département de Pharmacologie Moléculaire, Montpellier, France (M.A.A., D.M., V.B., L.P., J.P.P.); and CisBio International, Bagnols-sur-Cèze, France (M.F., H.A.)

Received August 28, 2006; accepted January 12, 2007

ABSTRACT

G protein-coupled receptors transmit extracellular signals into the cells by activating heterotrimeric G proteins, a process that is often followed by receptor desensitization. Monitoring such a process in real time and in living cells will help better understand how G protein activation occurs. Energy transfer-based approaches [fluorescence resonance energy transfer (FRET) and bioluminescence resonance energy transfer (BRET)] were recently shown to be powerful methods to monitor the G protein-coupled receptors (GPCRs)-G protein association in living cells. Here, we used a BRET technique to monitor the coupling between the protease-activated receptor 1 (PAR1) and Gα_{i1} protein. A specific constitutive BRET signal can be measured between nonactivated PAR1 and the Gα_{i1} protein expressed at a physiological level. This signal is insensitive to pertussis toxin (PTX) and probably reflects the preassembly of these two proteins. The BRET signal rapidly increases upon receptor activation in a PTX-sensitive manner. The BRET signal then returns to the basal level after few minutes. The desensitization of the BRET signal is concomitant with β-arrestin-1 recruitment to the receptor, consistent with the known rapid desensitization of PARs. The agonist-induced BRET increase was dependent on the insertion site of fluorophores in proteins. Taken together, our results show that BRET between GPCRs and Gα proteins can be used to monitor the receptor activation in real time and in living cells. Our data also revealed that PAR1 can be part of a preassembled complex with Gα_{i1} protein, resulting either from a direct interaction between these partners or from their colocalization in specific microdomains, and that receptor activation probably results in rearrangements within such complexes.

G protein-coupled receptors (GPCRs) represent one of the most important gene family in mammalian genomes. These receptors allow signals as diverse as photons, ions, amino acids, lipids, catecholamines, peptides, or proteins to transmit information inside the cells by activating heterotrimeric G proteins formed by various α, β, and γ subunits (Bockaert and Pin, 1999). However, the detailed analysis of GPCRs and G protein activation in living cells is still limited. Within the last few years, energy transfer technologies (FRET and BRET) were shown to enable such an analysis allowing to monitor the physical proximity between various partners of a GPCR signaling cascade: the receptor, G protein subunits, and their effectors (Janetopoulos et al., 2001; Bunemann et al., 2003; Yi et al., 2003; Azpiazu and Gautam, 2004; Frank et

This work was supported by grants from the Centre National de la Recherche Scientifique, Institut National de la Santé et de la Recherche Médicale, Universités de Montpellier 1 and 2, the Action Concertée Incitative "Biologie Cellulaire, Moléculaire et Structurale" of the French ministry of research and technology (grant BCMS328), the Agence Nationale de la Recherche (ANR-05-PRIB-02502), the European Community (grant LSHB-CT-200-503337), and CisBio International.

Article, publication date, and citation information can be found at http://molpharm.aspetjournals.org.

doi:10.1124/mol.106.030304.

ABBREVIATIONS: GPCR, G protein-coupled receptor; PAR, protease-activated receptor; BRET, bioluminescence resonance energy transfer; FRET, fluorescence resonance energy transfer; Rluc, *Renilla reniformis* luciferase; YFP, yellow fluorescent protein; TRAP, thrombin receptor-activating peptide; PTX, pertussis toxin; GABAb, γ-4-aminobutyric acid receptor type B; ELISA, enzyme-linked immunosorbent assay; SCH79797, *N*-3-cyclopropyl-7-{[4-(1-methyl-ethyl)phenyl]methyl}-7*H*-pyrrolo[3,2-f]quinazoline-1,3 diamine; DMEM, Dulbecco's modified Eagle's medium; PBS, phosphate-buffered saline; PCR, polymerase chain reaction; IGF, Institut de Génomique Fonctionnelle; TFLLR, Thr-Phe-Leu-Leu-Arg-NH_2; SLIGRL, Ser-Leu-Iso-Gly-Arg-Leu-NH_2; CGP54626, [*S*-(*R**,*R**)]-3-[[1-(3,4-dichlorophenyl)ethyl]amino]-2-hydroxypropyl](cyclohexylmethyl) phosphinic acid.

al., 2005; Galés et al., 2005, 2006; Hein et al., 2005; Nobles et al., 2005; Dowal et al., 2006; Rebois et al., 2006). Agonist-promoted energy transfer change has often been taken as the major indicator of either the association/dissociation of proteins or the transition from the inactive to active state of proteins. Indeed, although some authors linked the agonist-induced decrease of energy transfer signals with the reversible dissociation between G protein subunits (Janetopoulos et al., 2001; Yi et al., 2003; Azpiazu and Gautam, 2004), others proposed, in contrast, that no molecular dissociation occurred between α, β, and γ subunits after receptor activation, and the decrease in energy transfer signals reflects molecular rearrangements and conformational changes within the $\alpha\beta\gamma$ heterotrimer (Bunemann et al., 2003; Galés et al., 2006). Likewise, for the interaction between GPCRs and G proteins, some data are consistent with the association-dissociation model and the absence of receptor-G protein "preassociation" or "preassembly" (Hein et al., 2005), whereas others support a preassembly and agonist-induced conformational changes of preassembled GPCRs-G proteins complexes (Galés et al., 2005, 2006; Nobles et al., 2005).

Protease-activated receptors (PARs) are a family of four different receptors that are activated by various proteases (Macfarlane et al., 2001; Hollenberg and Compton, 2002). PAR1, PAR3, and PAR4 respond to a highly selective group of serine proteases that include thrombin, plasmin, the factor Xa, and the activated protein C (Macfarlane et al., 2001; Cottrell et al., 2002). In contrast, PAR2 receptor can be activated by trypsin, tryptase, and the coagulation factors VIIa and Xa (Macfarlane et al., 2001; Cottrell et al., 2002). The activation mechanism of these receptors involved the cleavage of their N-terminal segment by the protease, unmasking a new N terminus that acts as a tethered ligand, directly activating the transmembrane core of the receptor (Coughlin, 1999). Of interest, PARs can also be activated by synthetic peptides that mimic the tethered ligand without the requirement of protease cleavage of receptors (Vu et al., 1991; Chen et al., 1994; Al-Ani et al., 2002). Such an activation mechanism leads to the constitutive activation of the receptor by proteases, followed by the rapid desensitization, internalization, and degradation of the cleaved receptor (Cottrell et al., 2002; Trejo, 2003; Chen et al., 2004). This desensitization process involved the well-characterized phosphorylation of the receptor by G protein-coupled receptor kinases and the recruitment of arrestins (Paing et al., 2002; Trejo, 2003). PARs are involved in a number of physiological processes such as thrombosis (Chung et al., 2002), vascular biology (Barnes et al., 2004), inflammation (Kannan, 2002), and the regulation of cell proliferation and tumorigenesis (Boire et al., 2005) and represent important new targets for the treatment of a number of pathologies.

In the present study, we used a BRET approach to monitor the coupling between PAR1 and $G\alpha_{i1}$ protein in living COS-7 cells. Our data show that PAR1 receptor activation using either thrombin or agonist peptides mimicking the tethered ligands lead to a rapid but transient increase in the BRET signal measured between the receptor fused to yellow fluorescent protein (YFP) and $G\alpha_{i1}$ fused to *Renilla reniformis* luciferase enzyme (Rluc). The desensitization kinetic of this response is similar to that of the recruitment of β-arrestin-1 to the receptor, indicating that the observed signal reflects the G protein activation in living cells. It is interesting that our data also revealed a close proximity between the inactive receptor and the $G\alpha_{i1}$ protein consistent with their possible preassembly.

Materials and Methods

Materials. Human cDNAs for PAR1 and PAR2 were cloned into pcDNA3.1+ (Guthrie Research Institute, Sayre, PA); pcDNA3-Rluc, Rluc-β-arrestin-1, V2-YFP, and $G\alpha_{i1}$-122-Rluc were generously provided by R. Jockers, M. G. Scott (Institut Cochin, Paris, France), T. Durroux [Institut de Génomique Fonctionnelle (IGF), Montpellier, France], C. Galés, and M. Bouvier (Université de Montréal, Montreal, QC, Canada), respectively; bovine thrombin (~93 NIH U/mg of protein, 1 U/ml $\approx$ 0.3 μM) and bovine trypsin pancreas were from Calbiochem Merck KgaA (Darmstadt, Germany); mouse anti-PAR1 antibody was from Zymed Laboratories (South San Francisco, CA); monoclonal anti-Flag M2 was from Sigma-Aldrich (St. Louis, MO); the polyclonal rabbit anti-$G\alpha_{i1/2}$ antibody (Lledo et al., 1992) and TRAP-14 peptide (Ser-Phe-Leu-Leu-Arg-Asn-Pro-Asn-Asp-Lys-Tyr-Glu-Pro-Phe-NH_2) were generous gifts from Dr. V. Homburger (IGF, Montpellier, France); SCH79797, Thr-Phe-Leu-Leu-Arg-NH_2 (TFLLR), and Ser-Leu-Iso-Gly-Arg-Leu-NH_2 (SLIGRL) peptides were from Tocris Cookson Inc. (Ellisville, MO); 96-well white microplates were from Greiner Bio-One SAS (Courtaboeuf, France); and Coelenterazine *h* substrate was from Promega (Charbonnières, France).

Plasmid Constructions. PAR1-YFP and PAR2-YFP fusion proteins were obtained by fusing the cDNA coding for YFP at the C-terminal end of receptors. For this, the coding regions of the human PARs have been amplified without stop codon using forward and reverse primers bearing the cloning BamHI site. The PCR products were inserted in phase between BamHI site into pRK6-YFP plasmid (T. Durroux, IGF, Montpellier, France). Similar strategy has been followed for the truncation of the N terminus (PAR1-ΔN-YFP) and the deletion of the C terminus (PAR1-ΔC-YFP) of PAR1 using the BamHI cloning site. For all of these constructs, the junction sequence between PARs and YFP was similar coding for 10 residues (YRDPRVPVAT).

For $G\alpha_{i1}$-Rluc fusion protein, site-directed mutagenesis was first performed on the cDNA of the human $G\alpha_{i1}$ to insert an EcoRI site between position encoding isoleucine 93 and aspartic acid 94 within the helical domain of the G protein (Fig. 11C). Then, the intermediate construct ($G\alpha_{i1}$-EcoRI) was used to insert at the EcoRI site the coding region of Rluc without stop codon and bearing the glycine rich-linker sequences coding for Gly-Asn-Ser-Gly-Gly in the 5′ end and Gly-Gly-Gly-Asn-Ser in the 3′ end, respectively. The PCR product of Rluc was inserted in phase between the EcoRI site of $G\alpha_{i1}$-EcoRI plasmid. For $G\alpha_s$-Rluc construct, the fusion was performed between alanine 188 and aspartic acid 189 using NheI site with glycine rich-linker similar to that used for $G\alpha_{i1}$-Rluc.

For Flag-PAR1-YFP construct, the MluI/HindIII fragment of PAR1-YFP obtained by PCR was inserted between MluI and HindIII into pRK5-Flag-GABAb1 containing the mGluR5 signal peptide to allow its expression and targeting to the cell surface. All constructs were verified by sequencing, and their expression in COS-7 cells was confirmed by luminescence, fluorescence, and Western blot.

Cell Culture and Transfection. COS-7 cells were grown in complete medium [DMEM supplemented with 10% (v/v) fetal bovine serum, 4.5 g/l glucose, 100 U/ml penicillin, 0.1 mg/ml streptomycin, and 1 mM glutamine) (all from Invitrogen, Carlsbad, CA). Transient transfections were performed using electroporation as described previously (Brabet et al., 1998).

Microplate BRET Assay and Kinetics Analysis. Twenty-four hours after transfection, COS-7 cells were detached with PBS and 5 mM EDTA, washed three times with PBS, and resuspended in a suitable volume of PBS. Cells at a density of 2 to 5 $\times$ 10^4 cells/well were distributed in a 96-well microplate. Coelenterazine *h* substrate

was added at a final concentration of 5 μM in the total volume of 50 μl/well. Readings were then immediately performed after the addition of different ligands at room temperature and at 0.05- or 0.5-s intervals and during several minutes using the Mithras LB 940 plate reader (Berthold Biotechnologies, Bad Wildbad, Germany) that allows the sequential integration of light signals detected with two filter settings (Rluc filter, 485 ± 20 nm; and YFP filter, 530 ± 25 nm). For the kinetic studies, we used the injection system of the Mithras reader. Data were collected using the MicroWin2000 software (Berthold Biotechnologies), and BRET signal was expressed in milliBRET units of BRET ratio as described previously (Ayoub et al., 2002). For dose-response data, curves were fitted with a nonlinear regression and sigmoid dose-response equation using Prism software (GraphPad Software Inc., San Diego, CA).

The kinetics analysis of the ligand-induced BRET signal between $G\alpha_{i1}$-Rluc and PAR1-YFP was performed on two time windows. The activation kinetic was determined on a time window of 50 s after thrombin injection (window 1) corresponding to a phase during which the desensitization process was reduced. Likewise, the desensitization kinetic was determined on a time window from 5 to 15 min after thrombin injection (window 2). For the activation kinetics, the signal was fitted with GraphPad Prism software using the equation $Y = \text{Plateau} + (\text{Top}_{\text{window1}} - \text{Plateau}) \times (1 - \exp^{(-k \times (X - X_0))})$, in which $\text{Top}_{\text{window1}}$ corresponds to the maximal BRET signal reached after thrombin injection and X_0 is the time of thrombin injection. For the desensitization kinetics, the signal was fitted using the equation $Y = (\text{Top}_{\text{window2}} - \text{Bottom}) \times (1 - \exp^{-k \times X}) + \text{Bottom}$, in which $\text{Top}_{\text{window2}}$ corresponds to the BRET signal reached after 5 min of thrombin injection. For both equations, X is the time, plateau represents the basal BRET before thrombin injection, and bottom represents the mean BRET signal after 15 min. The halftime value ($t_{1/2}$) was calculated as the ratio 0.69/k.

For the kinetics of β-arrestin-1 translocation, thrombin-promoted BRET signal was fitted using the equation $Y = \text{Top} \times (1 - \exp^{(-k \times X)})$, in which Top corresponds to the maximal BRET signal and X is the time.

cAMP Assay. The determination of the cAMP accumulation in COS-7 cells was performed in 96-well microplates using the HTRF-cAMP Dynamic kit (CisBio International, Bagnols sur Cèze, France). In brief, cells were stimulated 30 min at 37°C with ligands in the presence or the absence of 10 μM forskolin in 50 mM phosphate buffer, pH 7.0, 0.2% bovine serum albumin, 0.02% NaN_3, and preservatives. The reaction was stopped by 50 mM phosphate buffer, pH 7.0, 1 M KF, and 1% Triton X-100 containing HTRF assay reagents: the Europium Cryptate-labeled anti-cAMP antibody and the XL665-labeled cAMP. The assay was incubated overnight at 4°C, and time-resolved FRET signals were measured 50 μs after excitation at 620 and 665 nm using a RubyStar instrument (BMG Labtechnologies, Champigny-sur-Marne, France).

Inositol Phosphate Measurements. The determination of the inositol phosphate 1 accumulation in COS-7 cells was performed in 96-wells microplates using the HTRF-IP-One kit (CisBio International). In brief, cells were stimulated for 30 min at 37°C with thrombin in the stimulation buffer (10 mM HEPES, 1 mM $CaCl_2$, 0.5 mM $MgCl_2$, 4.2 mM KCl, 146 mM NaCl, 5.5 mM glucose, and 50 mM LiCl, pH 7.4). The reaction was stopped by 50 mM phosphate buffer, pH 7.0, 1 M KF, and 1% Triton X-100 containing HTRF assay reagents: the Europium Cryptate-labeled anti-IP1 antibody and d2-labeled IP1. The assay was incubated overnight at 4°C, and time-resolved FRET signals were measured 50 μs after excitation at 620 and 665 nm using a RubyStar instrument.

ELISA. Twenty-four hours after transfection, COS-7 cells were fixed for 5 min at room temperature with 4% of paraformaldehyde and permeabilized or not for 5 min with 0.05% Triton X-100. Cells were then blocked with phosphate-buffered saline containing 1% fetal calf serum and incubated 30 min at room temperature with 1 μg/ml monoclonal anti-PAR1 or anti-Flag M2 antibodies. After washing steps, cells were incubated for 30 min with 0.5 μg/ml horseradish peroxidase-coupled anti-mouse secondary antibody (GE Healthcare, Chalfont St. Giles, Buckinghamshire, UK) and washed again. Bound antibody was detected using a SuperSignal substrate (Pierce, Rockford, IL) and a Mithras LB 940 plate reader.

Luciferase Gene Reporter Assay. COS-7 cells were transfected with the serum-response element-luciferase gene reporter and PAR1 receptors, washed with PBS, and switched to serum-free DMEM overnight. Cells were then treated or not with ligands for 6 h in the serum-free DMEM at 37°C, washed with PBS, and lysed with the reagent containing the luciferase substrate (Promega Bright-Glo Luciferase Assay System). Luminescence was measured immediately using the Mithras LB 940 instrument.

Ligand Binding Assay. Ligand binding assay was performed as described previously (Galvez et al., 2001) with 40,000 cells/well and using the radiolabled GABAb receptor antagonist [^{3}H]CGP54626 (specific activity = 40 Ci/mmol) at the final concentration of 5 nM. Specific binding was determined by the incubation of cells with GABA 1 mM and the number of receptors per well or per cell was determined and correlated with the ELISA signal using the anti-Flag antibody.

Western Blotting. COS-7 cells transfected or not with $G\alpha_{i1}$ or $G\alpha_{i1}$-Rluc were lysed in Laemmli buffer (125 mM Tris-HCl, pH 6.8, 4% SDS, 20% glycerol, and 0.01% bromphenol blue) and warmed for 5 min at 90°C. Samples were then resolved by 10% SDS-polyacrylamide gel electrophoresis, transferred to nitrocellulose membrane (GE Healthcare), and subjected to immunoblotting using a polyclonal rabbit anti-$G\alpha_{i1/2}$ antibody (Lledo et al., 1992). Immunoreactive bands were visualized by the ECL detection Kit (GE Healthcare) on Kodak ML light films.

Confocal Imaging. COS-7 cells transiently expressing PAR1-YFP were fixed for 5 min at room temperature with 4% paraformaldehyde and washed with PBS. Coverslips were then mounted with Gel/Mount (Biomeda, Foster City, CA) and microscopic observations were performed on a Leica SP2 UV (Leica, Wetzlar, Germany) confocal microscope with a Plan-Apochromat 63×/1.4 numerical aperture oil objective with the appropriate YFP spectrums sittings.

Statistical Analysis. Two-way analysis of variance test associated to Bonferroni post test (GraphPad Prism software) was used to determine statistically significant differences between control (in the absence of ligands) and stimulated conditions.

Results

PAR1 and $G\alpha_{i1}$ Protein Fused to Energy Acceptor and Donor Proteins. To monitor the coupling of PAR1 to $G\alpha_{i1}$ protein using a BRET approach, these two proteins were fused with the energy acceptor YFP and the energy donor Rluc, respectively (Fig. 1A). The YFP was fused at the C terminus of PAR1, and this did not alter its expression at the cell surface as shown by confocal microscopy (Fig. 1B) or ELISA assay with the anti-PAR1 antibody (Fig. 1C), showing that the majority of receptors is expressed on the cell surface. Functional analysis showed that PAR1-YFP activated signaling pathways in similar way than the wild-type receptor, as monitored by the inositol phosphate production (Fig. 1D), luciferase gene reporter, and cAMP assays (data not shown). Thrombin potency measured on cells expressing PAR1-YFP (EC_{50} = 1 ± 0.4 nM, n = 3) was similar to that measured on cell expressing PAR1 (EC_{50} = 1.68 ± 1.3 nM, n = 3).

The $G\alpha_{i1}$-Rluc was obtained by inserting Rluc within the helical domain of the $G\alpha_{i1}$ protein between Ile93 and Asp94 residues. Such a position was chosen based on the crystal structure of the $G\alpha\beta\gamma$ heterotrimeric complex and was already used in many other studies with either $G\alpha_i$ (Bunemann et al., 2003; Frank et al., 2005; Galés et al., 2006), $G\alpha_s$ (Yi et al., 2003; Hynes et al., 2004), or $G\alpha_o$ (Azpiazu and Gautam,

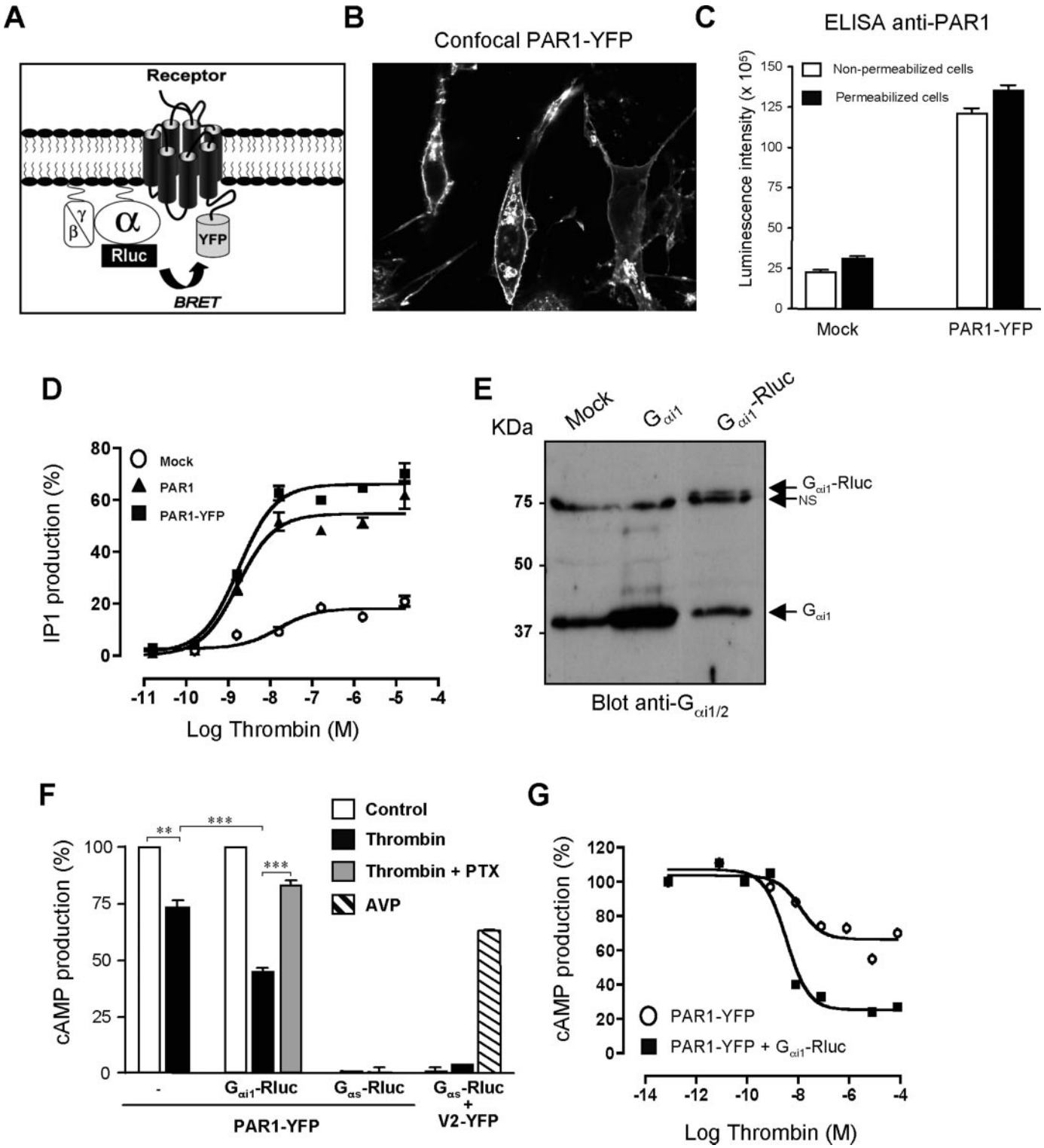

Fig. 1. Cell expression and functional analysis of PAR1-YFP and $G\alpha_{i1}$-Rluc fusion proteins. A, for BRET experiments, PAR1 and $G\alpha$ proteins ($G\alpha_{i1}$ and $G\alpha_s$) were fused to the YFP and Rluc, respectively, and transiently coexpressed in COS-7 cells as described under *Materials and Methods*. B, confocal microscopy on COS-7 cells transiently expressing PAR1-YFP. C, ELISA assay performed on cells expressing or not PAR1-YFP and permeabilized or not with Triton X-100 (0.05%) using the monoclonal anti-PAR1 antibody (1 μg/ml). D, inositol phosphate 1 production measured on cells expressing or not either PAR1 or PAR1-YFP and stimulated with increasing concentrations of thrombin. E, Western blotting on cells expressing or not $G\alpha_{i1}$ or $G\alpha_{i1}$-Rluc (3 μg of DNA each) using the anti-$G\alpha_{i1/2}$ antibody (1:1000); NS, nonspecific band. F, ligand-promoted intracellular cAMP modulation in cells expressing PAR1-YFP or V2-YFP in the absence or presence of either $G\alpha_{i1}$-Rluc or $G\alpha_s$-Rluc. The treatment with PTX (100 ng/ml) was performed overnight at 37°C before the cell stimulation and cAMP measurements. G, thrombin-promoted intracellular cAMP modulation in cells expressing PAR1-YFP in the absence or presence of $G\alpha_{i1}$-Rluc fusion protein. For cAMP assay, data represent the percentage of inhibition of forskolin-induced cAMP production. Data are representative of three independent experiments. ***, $p < 0.001$; **, $p < 0.01$ compared with control (in the absence of ligand).

2004; Nobles et al., 2005). In all cases, these fusion G proteins were shown to be correctly expressed and to allow an efficient coupling of receptors to their effectors. Indeed, like $G\alpha_{i1}$ (~43 kDa), our $G\alpha_{i1}$-Rluc is correctly expressed at the expected molecular mass (~78 kDa), as shown by Western blot using the antibody that recognizes $G\alpha_{i1}$ and $G\alpha_{i2}$ subunits (Fig. 1E) and by luminescence measurements (Fig. 2C). Note that the $G\alpha_{i1}$-Rluc expression level is close to that of the endogenous proteins. The functionality of $G\alpha_{i1}$-Rluc construct is illustrated by its ability to potentiate the inhibition of forskolin-stimulated cAMP production mediated by PAR1-YFP in a PTX-sensitive manner (Fig. 1F). In addition, the coexpression of $G\alpha_{i1}$-Rluc with PAR1-YFP (Fig. 1G), lysophosphatidic acid, or GABAb (data not shown) receptors largely enhanced agonist-induced inhibition of cAMP production. Such a potentiation in cAMP inhibition did not result from an increased expression level of PAR1 at the cell surface in the presence of the cotransfected $G\alpha_{i1}$ protein, as shown using an ELISA assay performed on intact cells using anti-PAR1 antibody (data not shown).

Monitoring PAR1-$G\alpha_{i1}$ Proximity in Living Cells by BRET. In cells coexpressing PAR1-YFP and $G\alpha_{i1}$-Rluc, a significant basal BRET signal was detected compared with cells coexpressing $G\alpha_s$-Rluc and PAR1-YFP or V2-YFP (Fig. 2, A and B). When cells were treated with thrombin (50 U/ml ≈ 15 μM), the BRET signal significantly increased between PAR1-YFP and $G\alpha_{i1}$-Rluc but not $G\alpha_s$-Rluc (Fig. 2A). In contrast, the BRET between $G\alpha_s$-Rluc and V2-YFP can be specifically increased after cell stimulation with vasopressin (1 μM) (Fig. 2B). These differences in the basal BRET signal and the sensitivity to receptor activation between $G\alpha_{i1}$-Rluc and $G\alpha_s$-Rluc were not due to the difference in the expression level of BRET partners quantified by luminescence and fluorescence measurements (Fig. 2C). These results are compatible with the coupling properties of PAR1 and V2 receptors illustrated in Fig. 1F, because PAR1 is known to activate $G\alpha_{i1}$ but not $G\alpha_s$ and inversely for V2.

The Specificity of the Basal and the Protease-Induced BRET Signal. To demonstrate the specificity of both the basal and agonist-induced BRET signal, we performed BRET-saturation assay developed previously to demonstrate the specificity of protein-protein interactions (Mercier et al., 2002; Ayoub et al., 2004). Indeed, when the amount of $G\alpha_{i1}$-Rluc was maintained constant, increasing the amount of PAR1-YFP leads to an increase in the BRET ratio that reaches a plateau (Fig. 3A). This plateau probably corresponds to the situation in which all $G\alpha_{i1}$-Rluc proteins available are specifically "preassembled" with available PAR1-YFP. Of interest, activation of the receptor leads to an increase in the maximal saturated BRET, consistent with a change in the energy transfer efficiency, rather than to the recruitment of additional G proteins in the vicinity of the receptor.

The specificity of the energy transfer was also verified by the BRET competition assay (Ayoub et al., 2002). The constitutive and thrombin-promoted BRET signals between PAR1-YFP and "nonsaturating" amount of $G\alpha_{i1}$-Rluc can be decreased by the coexpression of the untagged $G\alpha_{i1}$ protein (Fig. 3B). This was not due to the change in the acceptor/donor (YFP/Rluc) ratio controlled by measuring both luminescence (Rluc signal) and fluorescence (YFP signal) signals (Fig. 3C). This further confirms that the amount of $G\alpha_{i1}$ proteins in the vicinity of the receptor is saturable.

Quantification of PAR1 Expression at the Cell Surface. To determine the number of PAR1 receptors at the cell surface, we used a Flag-PAR1-YFP construct that possesses a Flag epitope inserted at the N terminus. This receptor was shown to share the same functional properties as the wild-type PAR1 in terms of its ability to activate the inositol phosphate formation (data not shown). ELISA assay revealed that the receptor is correctly targeted to the cell surface (Fig. 4A). By comparing the ELISA signal with Flag-PAR1-YFP with that measured with a Flag-GABAb receptor, for which the exact expression level can be determined by binding studies on intact cells with a nonpermeable radioligand (Fig. 4B), we calculated an expression of approximately 100,000 Flag-PAR1-YFP receptors per COS-7 cell. Fluorescence measurements indicate that Flag-PAR1-YFP receptor expression

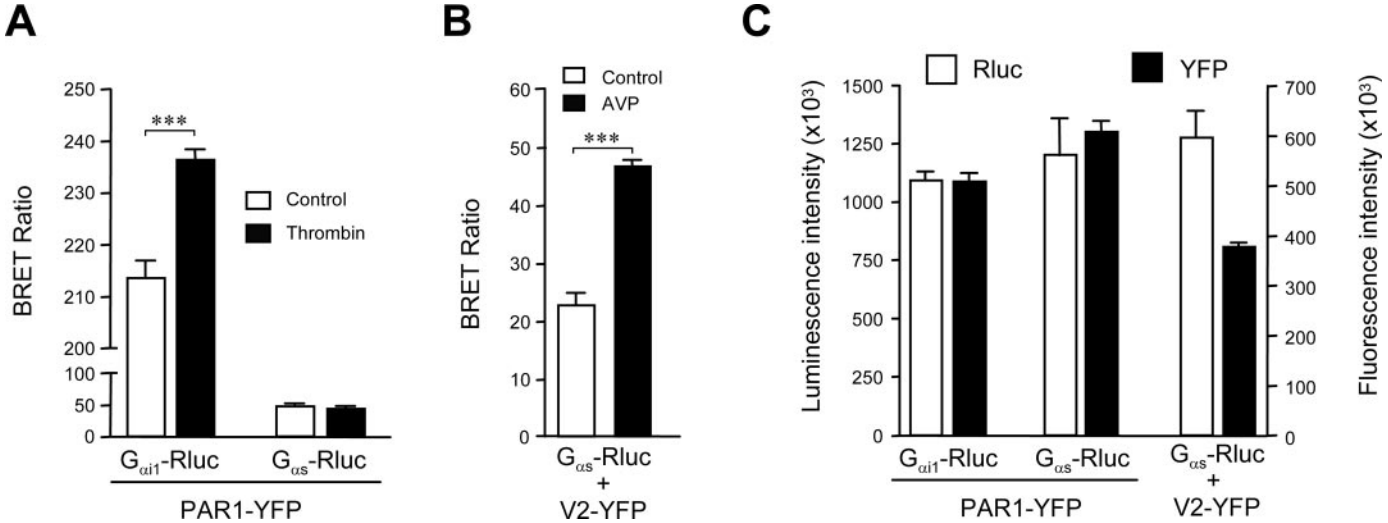

Fig. 2. Specific constitutive and thrombin-promoted BRET between PAR1 and $G\alpha_{i1}$ protein in living COS-7 cells. BRET measurements were performed on cells coexpressing $G\alpha_{i1}$-Rluc or $G\alpha_s$-Rluc with either PAR1-YFP (A) or V2-YFP (B) in the absence or presence of thrombin (50 U/ml ~ 15 μM) or arginine vasopressin (1 μM) as indicated. C, quantification of the luciferase (Rluc) activity (□) and YFP fluorescence (■) of BRET partners measured in BRET assay. Data are representative of three independent experiments. ***, $p < 0.001$; **, $p < 0.01$ compared with control (in the absence of ligand).

is 5 times lower than the PAR1-YFP under similar transfection conditions (Fig. 4C), such that the measured basal BRET between Flag-PAR1-YFP and $G\alpha_{i1}$-Rluc is also lower (Fig. 4D) but still within the BRET saturation curve, as indicated by the corresponding YFP/Rluc ratio (Fig. 3A).

Real-Time Analysis of PAR1-$G\alpha_{i1}$ Association and Desensitization. Kinetic analysis showed that thrombin-induced BRET increase between $G\alpha_{i1}$-Rluc and PAR1-YFP occurred rapidly ($t_{1/2}$ = 4.3 ± 0.6 s, n = 13) (Fig. 5A). This increase persists for a few minutes and returns to the basal signal 15 min after protease application (Fig. 5B), consistent with known PAR1 desensitization properties (Trejo, 2003). Indeed, when the signal was measured after preincubation for 30 min with thrombin, no BRET increase was observed (Fig. 5C). It is interesting that this decrease in agonist-induced BRET is concomitant with the recruitment of β-ar-

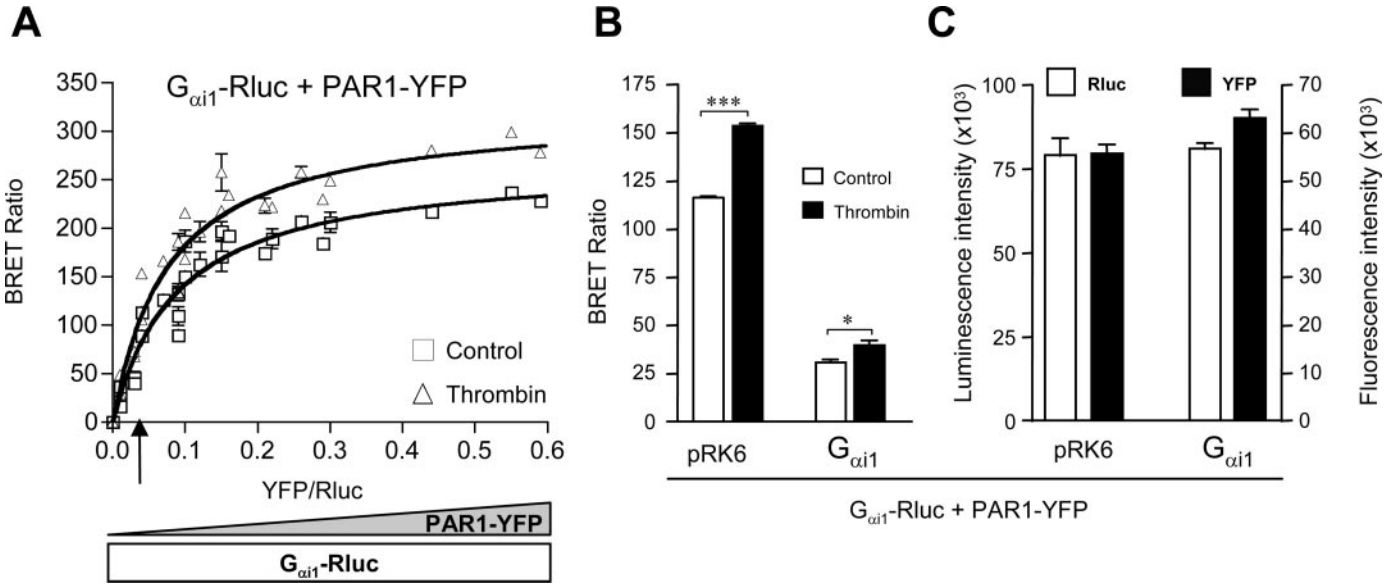

Fig. 3. BRET saturation and BRET competition assays of the BRET between PAR1 and $G\alpha_{i1}$. A, BRET saturation assay was performed on cells coexpressing constant amount of $G\alpha_{i1}$-Rluc fusion protein (energy donor) and increasing amounts of PAR1-YFP (energy acceptor) and BRET signal was determined in the absence (□) or presence (△) of thrombin (50 U/ml) and fitted with fluorescence/luminescence ratio (YFP/Rluc) using a nonlinear regression equation (GraphPad Prism software). The arrow indicates the Flag-PAR1-YFP/$G\alpha_{i1}$-Rluc ratio (~0.04) for which the receptor number has been determined by radiobinding assay and corresponding to 100,000 Flag-PAR1-YFP receptors/cell (see Fig. 4). B, BRET-competition assay was performed on cells transiently coexpressing $G\alpha_{i1}$-Rluc and PAR1-YFP with an excess of the untagged $G\alpha_{i1}$ protein and in the absence (□) or presence (■) of thrombin. C, quantification of the luciferase (Rluc) activity (□) and YFP fluorescence (■) measured in BRET competition assay. The saturation curve represents the mean ± S.E.M. of three individual experiments, and data shown in B and C are representative of three independents experiments. ***, $p < 0.001$.*, $p < 0.05$ compared with control (in the absence of thrombin) or with pRK6 (in the absence of the untagged $G\alpha_{i1}$).

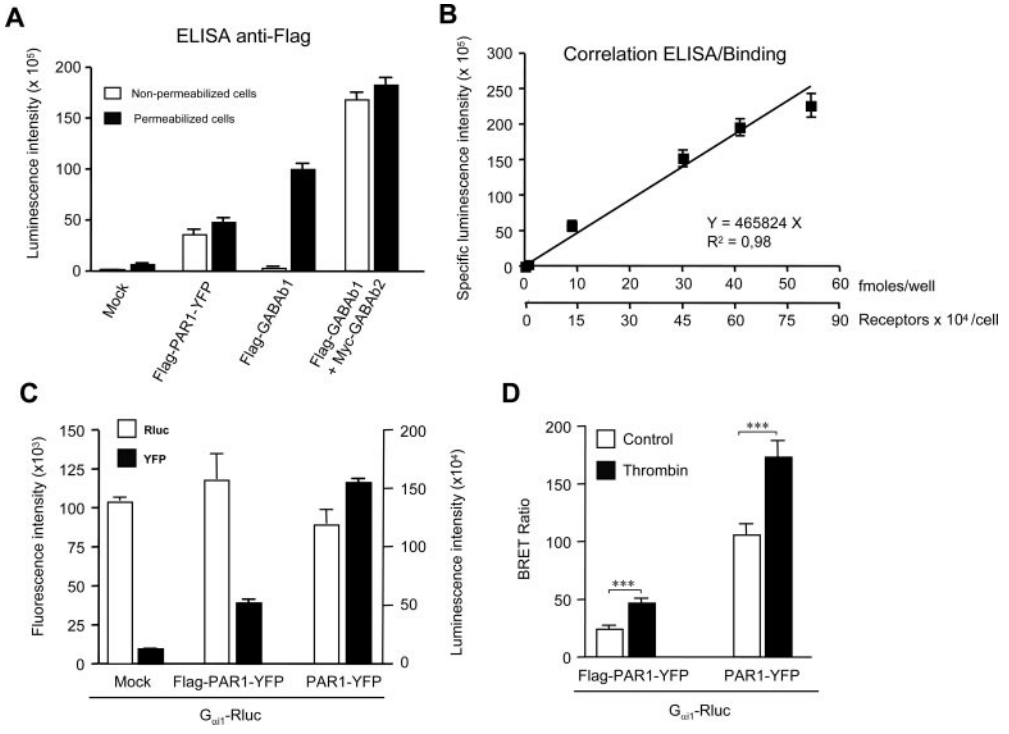

Fig. 4. Quantification of PAR1 expression at the cell surface. A, ELISA assay were performed on intact and permeabilized cells transiently expressing the indicated receptors using the anti-Flag antibody (1 μg/ml). B, correlation between the ELISA signal with Flag-GABAb receptor measured on nonpermeabilized cells and the receptor number determined by radiobinding assay as described under *Materials and Methods* section and represented as femtomoles of receptors per well or receptor number per cell. Cells transiently expressing $G\alpha_{i1}$-Rluc and either PAR1-YFP or Flag-PAR1-YFP were used to determine the relative expression level of $G\alpha_{i1}$-Rluc by luminescence (□) and receptors by fluorescence (■) (C) and to measure the energy transfer between the G protein and receptors in the absence or presence of thrombin (50 U/ml). Data are representative of at least three independent experiments. ***, $p < 0.001$ compared with control (in the absence of thrombin).

restin-1 to PAR1, also monitored by BRET. Indeed, thrombin application induced a BRET increase between Rluc-β-arrestin-1 and PAR1-YFP in a dose-dependent manner with a potency (EC_{50} = 2 ± 0.3 nM, n = 3) similar to that determined in other functional assays (Fig. 6A). Moreover, kinetic analysis shows that the $t_{1/2}$ value of the recruitment of β-arrestin-1 (5.4 ± 0.9 min, n = 5) (Fig. 6B) is compatible with that of the decay phase of agonist-induced BRET between $G\alpha_{i1}$-Rluc and PAR1-YFP ($t_{1/2}$ = 6.9 ± 1.7 min, n = 8, assuming a monoexponential decay) (Fig. 5B). These data demonstrate that a fast and reversible process is involved in the increase in BRET between PAR1 and $G\alpha_{i1}$ resulting from receptor activation, and the activation/desensitization processes of PAR1 can be studied by BRET.

PARs Activation Is Responsible for the Increase in the BRET Signal. Several lines of evidence indicate that thrombin-induced BRET increase results from PAR1 activation. First, when using a trypsin-activated PAR2 receptor (Coughlin, 2000; Macfarlane et al., 2001) fused to YFP instead of PAR1, a similar basal BRET was measured with $G\alpha_{i1}$-Rluc that is increased after trypsin (100 nM) but not thrombin stimulation (Fig. 7A). Second, thrombin (Fig. 7B) and trypsin (Fig. 7C) effects on PAR1 and PAR2, respectively, were dose-dependent with EC_{50} values (6.3 ± 0.2 nM, n = 17, and 1.3 ± 0.3 nM, n = 3, respectively) comparable with potencies reported for these proteases on PARs (O'Brien et al., 2000; Al-Ani et al., 2002; Boire et al., 2005). Third, peptides known to mimic the activating N-terminal end of PARs after their cleavage by proteases increased the BRET signal. This was obtained either with the nonselective PAR-activating peptide TRAP-14 (100 μM) (Debeir et al., 1996) or with the PAR1-selective (TFLLR, 100 μM) (Chung et al., 2002) agonist peptides on PAR1-expressing cells (Fig. 8A). The PAR2-selective peptide (SLIGRL, 100 μM) (Al-Ani et al., 2002) had no effect on PAR1-expressing cells (Fig. 8A), but it was active on PAR2 expressing cells (data not shown). The TFLLR-induced BRET increase was dose-dependent with an EC_{50} value of 5.8 ± 1.9 μM (n = 8) in agreement with its reported potency on PAR1 (Fig. 8B) (Seeley et al., 2003). Like for thrombin, kinetics analysis shows that peptide-induced BRET increase occurs rapidly ($t_{1/2}$ = 6.5 ± 1.5 s, n = 5) (Fig. 8C). Similar effect of the PAR1-selective peptide was observed when PAR1 was deleted of its N-terminal end containing the tethered ligand (PAR1-ΔN-YFP) (Fig. 8D) and making the receptor insensitive to thrombin (Fig. 8, E and F).

Finally, both protease inhibitors (Fig. 9A) and the PAR1-selective nonpeptidic antagonist SCH79797 (10 μM) (Fig. 9B) completely abolished the agonist-promoted BRET increase without affecting the basal BRET signal.

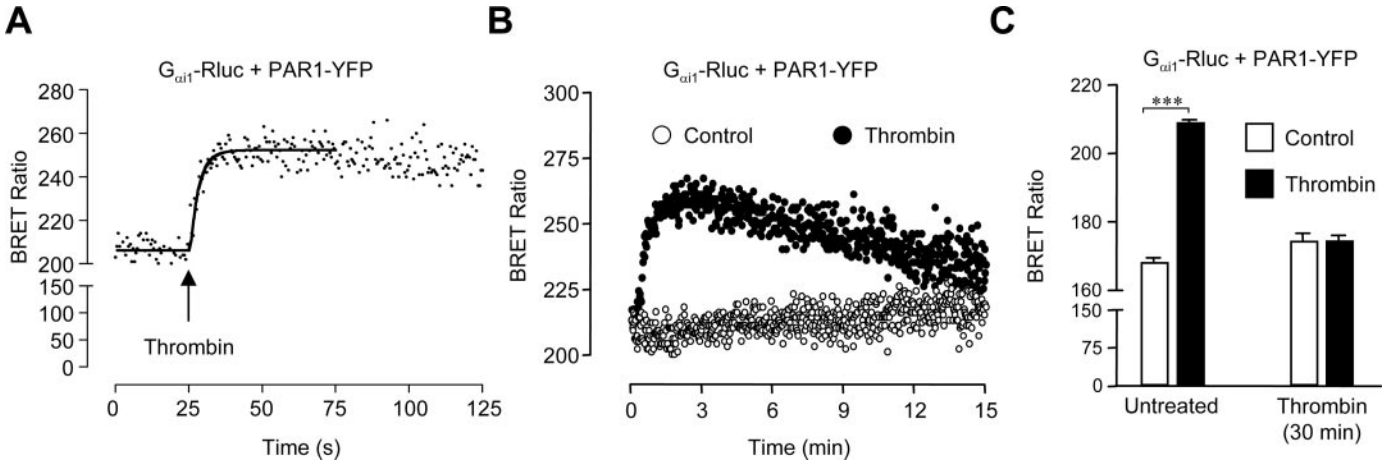

Fig. 5. Kinetic analysis of thrombin-induced BRET increase between PAR1 and $G\alpha_{i1}$. Cells transiently coexpressing $G\alpha_{i1}$-Rluc and PAR1-YFP were used for BRET experiments, and repetitive signals were recorded immediately before and after the injection of thrombin (50 U/ml) during 125 s (A) or 15 min (B). For A, BRET signal was fitted as described under *Materials and Methods*. C, cells transiently coexpressing $G\alpha_{i1}$-Rluc and PAR1-YFP were pretreated or not with thrombin 30 min at 37°C, and BRET measurements were then performed immediately after stimulation (■) or not (□) with thrombin. Data are representative of 13 (A), 8 (B), and 3 (C) independent experiments. ***, $p < 0.001$ compared with control (in the absence of thrombin).

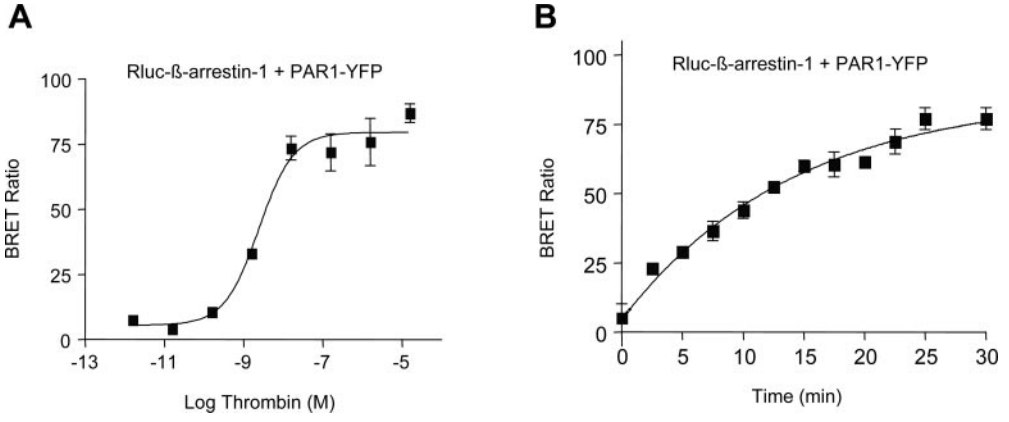

Fig. 6. Thrombin-induced β-arrestin-1 recruitment to PAR1 monitored by BRET. For BRET experiments on COS-7 cells transiently expressing Rluc-β-arrestin-1 and PAR1-YFP, cells were pretreated either 30 min at 37°C with increasing concentrations of thrombin (A) or with 50 U/ml ~15 μM concentration of thrombin at the indicated time (B). For B, the kinetic analysis is described under *Materials and Methods*. Data are representative of three (A) or five (B) independent experiments.

Agonist-Induced BRET Increase Is Associated to $G\alpha_{i1}$ Activation. We next examined whether the basal and agonist-induced BRET result from G protein activation. Inactivating $G\alpha_{i1}$-Rluc with PTX (100 ng/ml) (Fig. 10) suppressed agonist-induced BRET but not the basal signal. This demonstrates that the basal BRET measured in the absence of PAR1 activation does not result from G protein activation. Moreover, these data reveal that the mode of interaction or

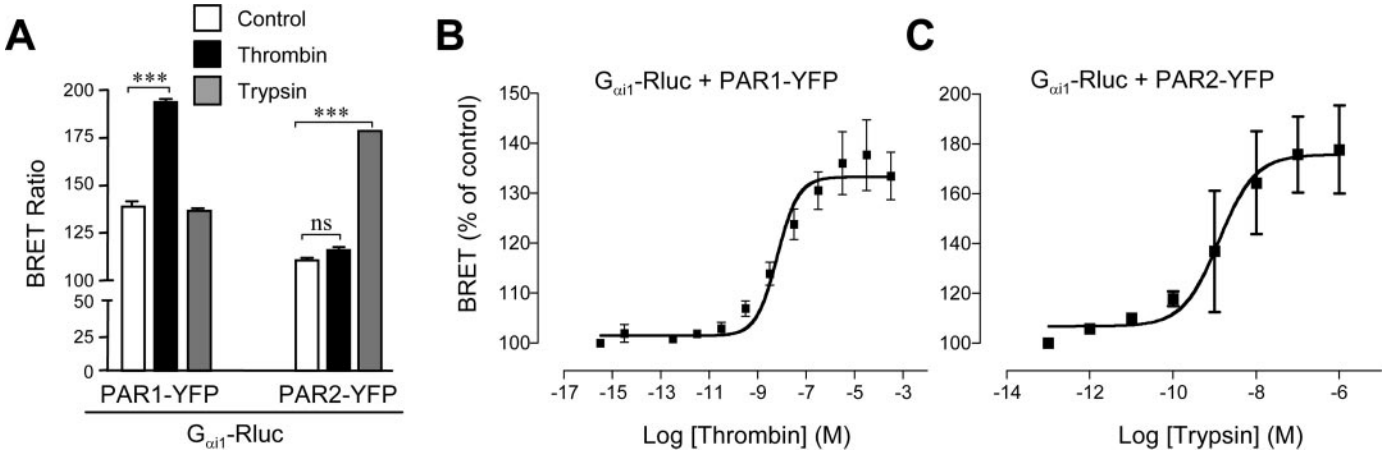

Fig. 7. The BRET increase is receptor- and protease-specific. A, the $G\alpha_{i1}$-Rluc fusion protein was transiently coexpressed with PAR1-YFP or PAR2-YFP as indicated, and energy transfer measurements were performed at 25°C immediately after stimulation or not with thrombin (50 U/ml) or trypsin (100 nM). Dose-response experiments of thrombin (B) or trypsin (C) -induced BRET increase between $G\alpha_{i1}$ protein and PARs as indicated. Data are mean ± S.E.M. of 6 (A), 17 (B), or 3 (C) independent experiments. ***, $p < 0.001$. ns, $p > 0.05$ compared with control (in the absence of ligands).

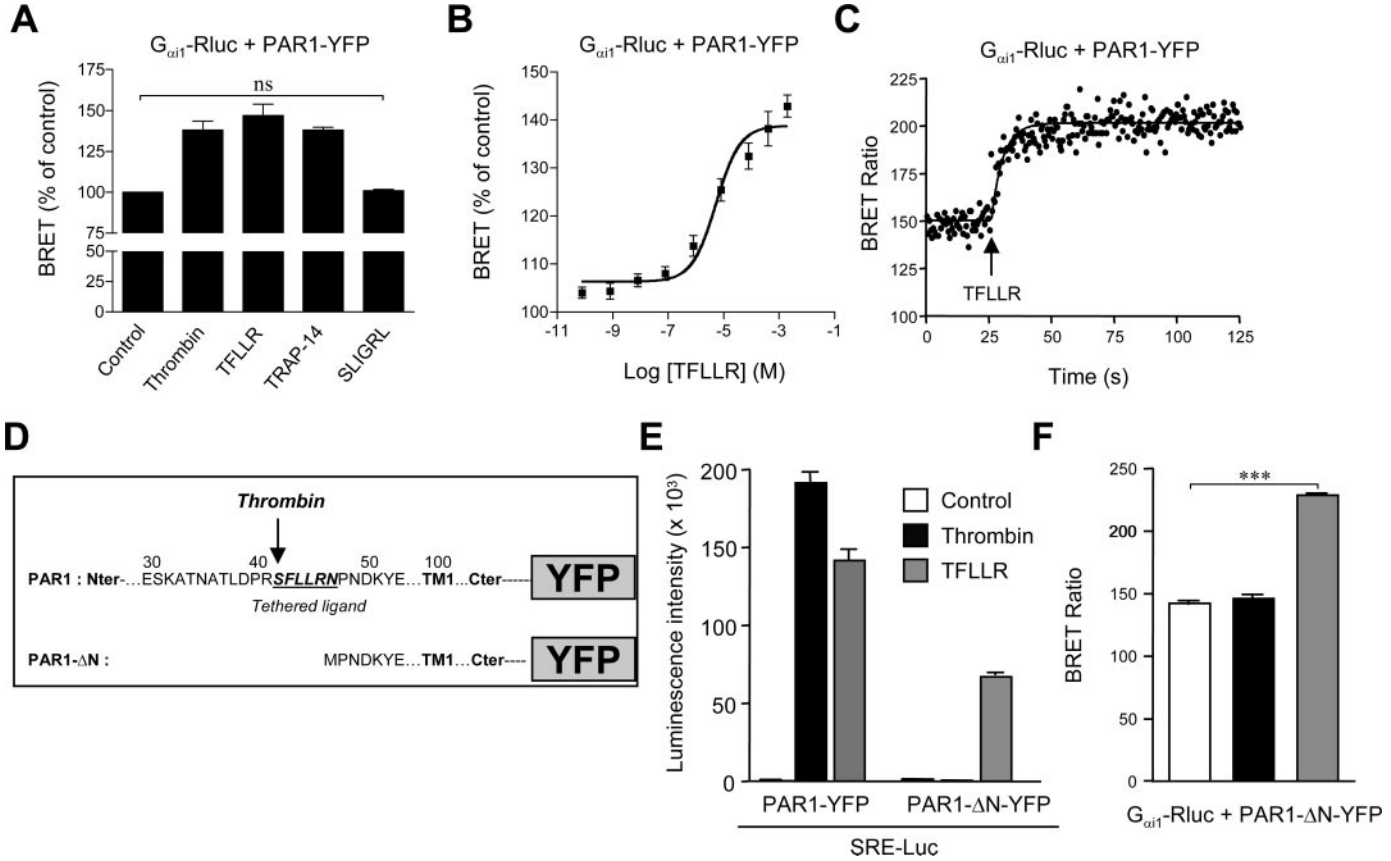

Fig. 8. Thrombin-induced BRET increase can be mimicked by PAR peptides. A, cells transiently coexpressing $G\alpha_{i1}$-Rluc and PAR1-YFP were used for BRET experiments after the rapid stimulation with thrombin (50 U/ml) or peptides (TFLLR, TRAP-14, SLIGRL) (100 μM) as indicated. B, dose-response of TFLLR-induced BRET increase. C, kinetics analysis of TFLLR-induced BRET increase between $G\alpha_{i1}$-Rluc and PAR1-YFP. D, schematic sequence of PAR1-ΔN-YFP mutant in which the thrombin cleavage site and the tethered ligand were deleted. E, luciferase gene reporter assay was performed on cells transfected with the serum-response element-luciferase gene reporter plasmid with either PAR1-YFP or PAR1-ΔN-YFP and treated for 6 h at 37°C with thrombin (50 U/ml) or the TFLLR peptide (100 μM) as indicated. F, BRET measurements on cells transiently coexpressing $G\alpha_{i1}$-Rluc and PAR1-ΔN-YFP in the absence or presence of thrombin (50 U/ml) or the TFLLR peptide (100 μM) as indicated. Data are the mean ± S.E.M. of three (A) or eight (B) independent experiments. For C, E, and F, data are representative of five, three, and three independent experiments, respectively. ***, $p < 0.001$. ns, $p > 0.05$ compared with control (in the absence of ligands).

assembly between $G\alpha_{i1}$ and PAR1 (the distance and/or the relative orientation of Rluc and YFP fused to $G\alpha_{i1}$ and PAR1, respectively) is probably different whether the receptor is in its inactive or active state.

Movement within the Preassembled PAR1-$G\alpha_{i1}$ Complexes Represents the Major Cause of the Agonist-Induced BRET Increase. To get more insights in the molecular events leading to BRET increase after receptor activation, similar experiments were conducted with a receptor in which the YFP was inserted at a different site, closer to the helix 8 (PAR1-ΔC-YFP) (Fig. 11A). Indeed, if the increase in BRET resulting from receptor activation is due to the recruitment of additional $G\alpha_{i1}$ protein in the close vicinity of the receptor, this should be observed regardless of the YFP position on the receptor. Such a deletion completely abolished the agonist-induced recruitment of β-arrestin-1 but not its ability to activate G proteins (data not shown). A high basal BRET signal was measured between PAR1-ΔC-YFP and $G\alpha_{i1}$-Rluc, but the activation of this mutant with either thrombin or TFLLR did not lead to any change in the BRET signal (Fig. 11B).

We also examined the influence of the Rluc position in $G\alpha_{i1}$ protein on the basal and agonist-induced BRET. For this reason, we used a $G\alpha_{i1}$ fusion protein in which Rluc was inserted at position Ala121–Glu122 in the helical-rich domain ($G\alpha_{i1}$-122-Rluc) (Galés et al., 2006). In this construct, the Rluc is positioned on the other side of the G protein compared with $G\alpha_{i1}$-Rluc used so far in our study (Fig. 11C). As shown in Fig. 11D, a larger basal BRET is observed with both PAR1-YFP and PAR1-ΔC-YFP and $G\alpha_{i1}$-122-Rluc compared with $G\alpha_{i1}$-Rluc (Fig. 11B), and this despite a similar expression level of all partners (data not shown). However, no further increase in BRET was observed upon activation of the receptors with either thrombin or TFLLR (Fig. 11D). Taken together, these data clearly dissociate the BRET increase from the recruitment of the G protein by the activated receptor and support the proposal that PAR1 and $G\alpha_{i1}$ are preassembled and that receptor activation led to a change in the positioning of the $G\alpha_{i1}$ subunit relative to the receptor.

Discussion

The application of energy transfer-based assays to study the interaction between GPCRs and their cognate G proteins constitutes an attractive field of research in GPCR biology. Here, we monitored the physical proximity between PAR1 and $G\alpha_{i1}$ protein using a BRET approach in living COS-7 cells. Our data show that the kinetics of BRET changes resulting from PAR1 receptor activation is consistent with the fast activation process and the known desensitization properties of these receptors. These data further indicate that BRET signals measured between the receptor and G protein can be used to monitor GPCR activation and desensitization in real time and in living cells.

Our data first revealed a significant basal BRET signal between PARs-YFP (PAR1 and PAR2) and $G\alpha_{i1}$-Rluc. This basal BRET is specific because it was not observed with $G\alpha_s$-Rluc, in agreement with the known coupling properties of PARs (Coughlin, 2000; Macfarlane et al., 2001), and is saturable as shown by the BRET-saturation experiment and the displacement by the "unlabeled" $G\alpha_{i1}$ protein. Moreover, such a basal BRET is measured with $G\alpha_{i1}$-Rluc expression level similar to that of endogenous $G\alpha_{i1}$ and is observed for receptor expression level at the cell surface of approximately 100,000 receptors per COS-7 cell. This is consistent with the known physiological expression of PAR1 in platelets [approximately 1000 receptors per platelet (Brass et al., 1992; Norton et al., 1993), corresponding to 100,000 receptors per COS-7 cell, assuming the latter is 10 times larger in diameter].

Recent studies using BRET or FRET approaches also reported a constitutive energy transfer between GPCRs and G proteins (Janetopoulos et al., 2001; Bunemann et al., 2003; Yi et al., 2003; Azpiazu and Gautam, 2004; Frank et al., 2005; Galés et al., 2005, 2006; Hein et al., 2005; Nobles et al., 2005). The authors propose that this is due either to the existence of a "preassociated" or "preassembled" receptor-G protein complexes or to the constitutive activity of the GPCR. Our data do not support that the basal BRET signal results from any possible constitutive activation of $G\alpha_{i1}$ by PARs. Indeed, there is so far no evidence for the constitutive activity of PARs, including in our expression system (data not shown). Moreover, PAR1 antagonist does not inhibit the basal BRET, and PTX did not affect the basal BRET, whereas it clearly prevents the agonist-induced increase in BRET. This firmly demonstrates that the basal BRET does not result from the activation of $G\alpha_{i1}$.

An increasing number of recent publications using BRET or FRET techniques reported the study of the physical prox-

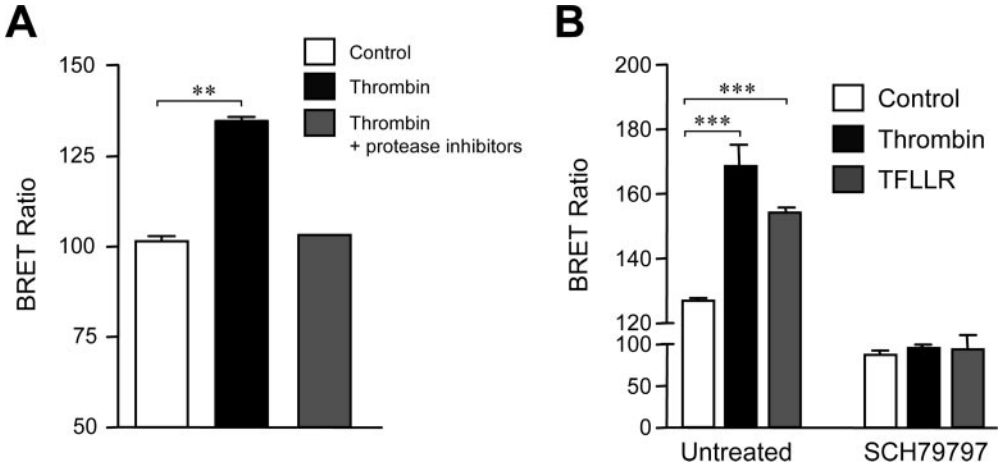

Fig. 9. Agonist-induced BRET increase is associated with the receptor activation. BRET measurements were performed in the absence or presence of thrombin or the TFLLR peptide on cells transiently coexpressing $G\alpha_{i1}$-Rluc and PAR1-YFP and pretreated or not for 15 min at room temperature with a mixture of protease inhibitors (A) or for 3 h at 37°C with the PAR1-selective antagonist SCH79797 (10 μM) (B). Data are representative of three independent experiments. ***, $p < 0.001$; **, $p < 0.01$ compared with control (in the absence of ligands).

imity between various partners of a GPCR signaling cascade: the receptor, G proteins, and their effectors (Janetopoulos et al., 2001; Bunemann et al., 2003; Yi et al., 2003; Azpiazu and Gautam, 2004; Frank et al., 2005; Galés et al., 2005, 2006; Hein et al., 2005; Nobles et al., 2005; Dowal et al., 2006; Rebois et al., 2006). Such a close proximity suggests a direct interaction between these partners. However, despite major efforts, we have not been able to observe coimmunoprecipitation of PARs and $G\alpha_{i1}$ protein. Although the direct interaction between PARs and $G\alpha_{i1}$ is a likely explanation, our data may also well be explained by a colocalization of both partners in specific small microdomains. Indeed, recent studies using single-molecule tracking reported that GPCR diffusion is restricted to small microdomains that may be limited by specific fences under the plasma membrane (Kusumi et al., 2005; Suzuki et al., 2005) or may possibly correspond to caveolae or lipid raft (Insel et al., 2005; Meyer et al., 2006). If the G proteins are also incorporated into such microdomains, this will probably result in a limited number of G proteins in the close vicinity of the receptor, consistent with a saturable basal BRET signal observed. Moreover, the likely high density of both receptors and G proteins in such microdomains (Insel et al., 2005) may favor energy transfer between Rluc and YFP fused to these partners. Other recent study by BRET and bimolecular fluorescence complementation approaches reported that receptors and G proteins complexes are formed early during proteins biosynthesis (Dupre et al., 2006), such that part of the basal BRET observed probably reflects such preformed intracellular complexes. However, it is worth noting that the basal BRET cannot result solely from intracellular complexes, as demonstrated by the BRET saturation experiment shown in Fig. 3A. The proportion of intracellular receptors is expected to increase when receptor expression levels reach saturation. If the basal BRET only reflects intracellular complexes, then the basal BRET value relative to the agonist-induced BRET value should largely increase with receptor expression. This is clearly not the case.

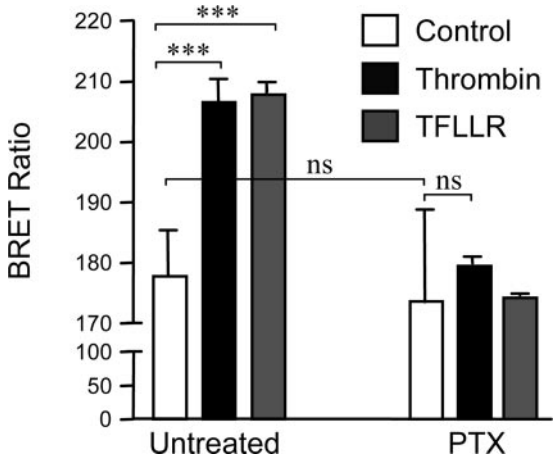

Fig. 10. Agonist-induced BRET increase is associated with $G\alpha_{i1}$ protein activation. BRET measurements were performed in the absence or presence of thrombin or the TFLLR peptide on cells transiently coexpressing $G\alpha_{i1}$-Rluc and PAR1-YFP and pretreated or not overnight at 37°C with pertussis toxin (100 ng/ml). Data are representative of three independent experiments. ***, $p < 0.001$. ns, $p > 0.05$ compared with control (in the absence of ligands or PTX).

Our second main observation is that PAR1 activation using either thrombin or peptides mimicking the tethered ligand

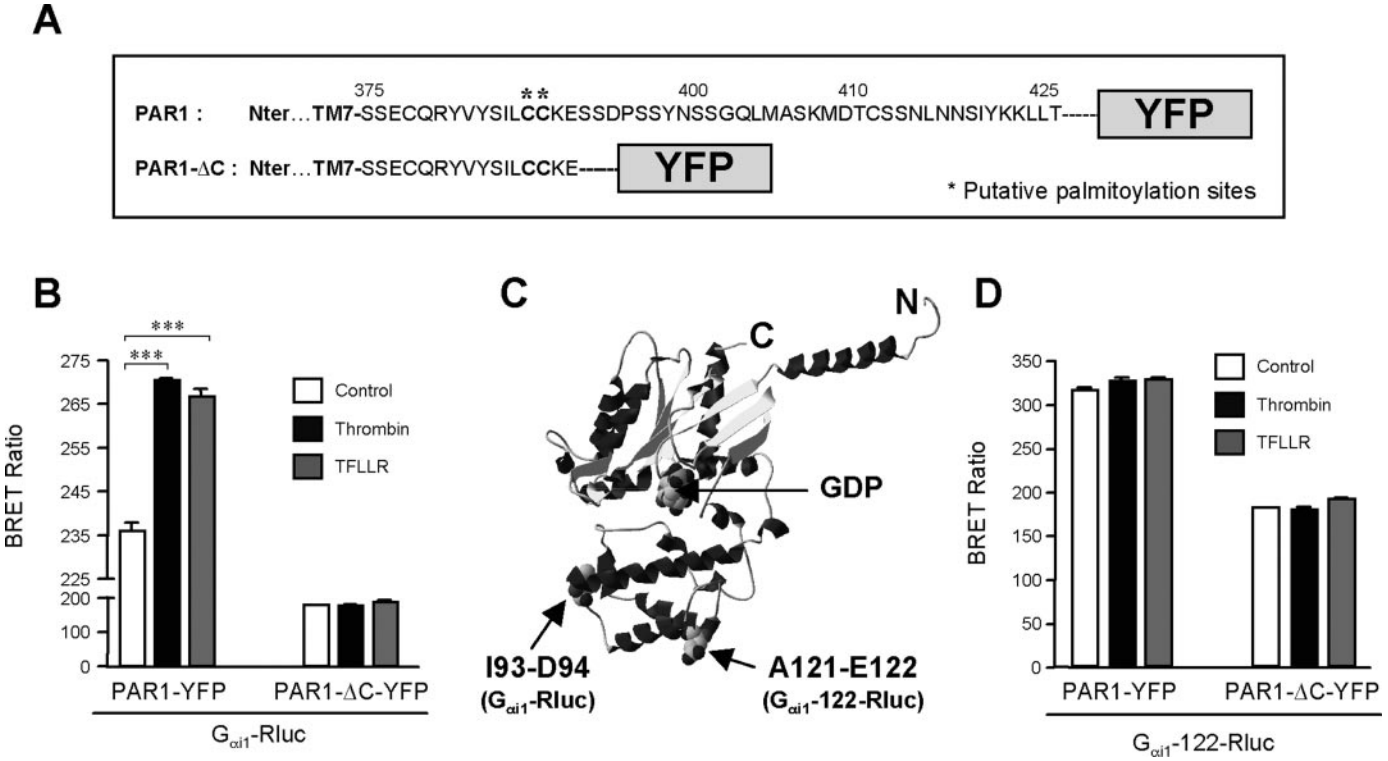

Fig. 11. The BRET increase depends on the position of Rluc and YFP within the preassembled PAR1-$G\alpha_{i1}$ complexes. A, schematic sequence of the YFP fusion protein of the C terminus-deleted PAR1 (PAR1-ΔC-YFP). BRET measurements were than performed in the absence or presence of thrombin or the TFLLR peptide on cells transiently coexpressing $G\alpha_{i1}$-Rluc (B) or $G\alpha_{i1}$-122-Rluc (D) with either PAR1-YFP or PAR1-ΔC-YFP as indicated. C, structural representation of the $G\alpha_{i1}$-GDP subunit (Protein Data Base code 1GP2) indicating the insertion sites of Rluc within the helical domain of the G protein. Data are representative of three independent experiments. ***, $p < 0.001$ compared with control (in the absence of ligands).

leads to a rapid increase in the BRET signal measured between the receptor and $G\alpha_{i1}$. These effects were specific to the receptor-protease/peptide pair. Moreover, the BRET increase was completely prevented by protease inhibitors, PAR1 antagonist, and PTX, indicating that agonist-induced BRET increase reflects the activation of receptor-G protein complexes. The agonist-induced BRET increase between $G\alpha_{i1}$-Rluc and PAR1-YFP was found to be rapid, in agreement with the rapid activation of G proteins by other GPCRs (Bunemann et al., 2003; Galés et al., 2005, 2006) and consistent with what is expected for such a process. Our kinetic analysis revealed a $t_{1/2}$ value of approximately 5 s when using saturating concentrations of thrombin, a process that seems slower than that reported for $G\alpha_i$ activation by the α_2-adrenergic receptor using either BRET (Galés et al., 2005; Galés et al., 2006) or FRET (Hein et al., 2005). This may well result from differences in the activation kinetic between different GPCRs, as observed between the PTH and α_2-adrenergic receptors (Vilardaga et al., 2003).

Further evidence that ligand-induced BRET increase results from G protein activation comes from the reversibility of this effect, consistent with the well-known PAR1 receptor desensitization (Trejo, 2003). Indeed, our data revealed that the agonist-induced BRET was largely decreased after 10 min and disappeared after 30 min, a kinetic that nicely fits with that of thrombin-induced β-arrestin-1 recruitment, also monitored by BRET. These data clearly indicate that agonist-induced BRET increase, but not the basal signal, is associated with PAR1 and $G\alpha_{i1}$ protein activation and further confirms the role of β-arrestin-1 in G protein uncoupling and PAR1 desensitization.

Two possibilities can explain the increase in BRET ratio observed between PARs and $G\alpha_{i1}$ protein after activation: 1) additional recruitment of $G\alpha_{i1}$ protein by the active form of the receptor; or 2) a change in the relative positioning of the fused YFP and Rluc within the preassembled receptors and G proteins. Our data are not consistent with the additional recruitment of $G\alpha_{i1}$ proteins in the preassembled complexes. Indeed, when increasing the amount of PAR1-YFP fusion protein with a constant amount of $G\alpha_{i1}$-Rluc, a saturation limit in the basal BRET signal is observed suggesting that all receptors are preassembled with the G protein under these conditions. Upon receptor activation, this maximal BRET value is increased. This is consistent with a better efficacy in the energy transfer within the preassembled receptor-G protein complex after activation rather than an increase in the number of G proteins interacting with the receptor. Accordingly, the increase in BRET signal observed after receptor activation probably results from a relative movement of the fused Rluc and YFP in the preassembled complexes. This proposal is also supported by the differential sensitivity to PTX treatment of the basal and agonist-induced BRET. Because a direct interaction between the C-terminal tail of $G\alpha_{i1}$ protein (the target of PTX) and the second and third intracellular loops of the receptor is known to occur during activation (Bourne, 1997), this further indicates that $G\alpha_{i1}$ interacts in a specific manner with the active form of the receptor. Moreover, the movement hypothesis is supported by the fact that the agonist-induced BRET change largely depends on the relative positioning of the Rluc and YFP in the G protein and the receptor, respectively. Indeed, the agonist-induced BRET increase is completely abolished when the YFP is fused closer to the helix 8 of PAR1 (in agreement with the expected movement of the C-terminal tail of the receptor during activation) (Fig. 11B) and is not observed if Rluc is inserted on the other side of the $G\alpha_{i1}$ protein (Fig. 11, C and D). This would not be expected if the increase in BRET simply results from G protein recruitment in the vicinity of the activated receptor.

Taken together, our data are consistent with a preassembly between $G\alpha_{i1}$ protein and PARs and their relative movement occurring after receptor activation. Whether such a preassembly results from a direct interaction of PARs and the G protein or their colocalization in small and saturable membrane microdomains remains to be further studied. Whatever, this is compatible with recent studies reporting the existence of preassembled complexes between receptors, G proteins and effectors (Galés et al., 2005, 2006; Nobles et al., 2005; Dowal et al., 2006; Rebois et al., 2006). All of these studies proposed that energy transfer changes reflect conformational changes within the preassociated complexes rather than receptor activation-promoted association. This suggests that the assembly of GPCRs, G proteins, and effectors does not represent a limiting step in the activation process and further documents the hypothesis that these partners can be part of preassembled protein complexes responsible for GPCR-mediated signaling, offering the way to a higher selectivity and a faster process.

Acknowledgments

We thank Drs. J C. Nicolas and A. Pillon (Institut National de la Santé et de la Recherche Médicale U540, Montpellier, France) for allowing us to use the Mithras reader and Drs. V. Homburger (IGF, Montpellier, France), R. Jockers, and M. G. Scott (Institut Cochin, Paris, France) for the provided materials. We also thank Drs. E. Trinquet (CisBio International, Bagnol-sur-Cèze, France) and T. Durroux (IGF, Montpellier, France) for constant support and M. Bouvier and C. Galés (Univeristé de Montréal, Montreal, QC, Canada) for helpful discussions.

References

Al-Ani B, Wijesuriya SJ, and Hollenberg MD (2002) Proteinase-activated receptor 2: differential activation of the receptor by tethered ligand and soluble peptide analogs. *J Pharmacol Exp Ther* **302:**1046–1054.

Ayoub MA, Couturier C, Lucas-Meunier E, Angers S, Fossier P, Bouvier M, and Jockers R (2002) Monitoring of ligand-independent dimerization and ligand-induced conformational changes of melatonin receptors in living cells by bioluminescence resonance energy transfer. *J Biol Chem* **277:**21522–21528.

Ayoub MA, Levoye A, Delagrange P, and Jockers R (2004) Preferential formation of MT1/MT2 melatonin receptor heterodimers with distinct ligand interaction properties compared with MT2 homodimers. *Mol Pharmacol* **66:**312–321.

Azpiazu I and Gautam N (2004) A fluorescence resonance energy transfer-based sensor indicates that receptor access to a G protein is unrestricted in a living mammalian cell. *J Biol Chem* **279:**27709–27718.

Barnes JA, Singh S, and Gomes AV (2004) Protease activated receptors in cardiovascular function and disease. *Mol Cell Biochem* **263:**227–239.

Bockaert J and Pin JP (1999) Molecular tinkering of G protein-coupled receptors: an evolutionary success. *EMBO (Eur Mol Biol Organ) J* **18:**1723–1729.

Boire A, Covic L, Agarwal A, Jacques S, Sherifi S, and Kuliopulos A (2005) PAR1 is a matrix metalloprotease-1 receptor that promotes invasion and tumorigenesis of breast cancer cells. *Cell* **120:**303–313.

Bourne HR (1997) How receptors talk to trimeric G proteins. *Curr Opin Cell Biol* **9:**134–142.

Brabet I, Parmentier ML, De Colle C, Bockaert J, Acher F, and Pin JP (1998) Comparative effect of L-CCG-I, DCG-IV and gamma-carboxy-L-glutamate on all cloned metabotropic glutamate receptor subtypes. *Neuropharmacology* **37:**1043–1051.

Brass LF, Vassallo RR Jr, Belmonte E, Ahuja M, Cichowski K, and Hoxie JA (1992) Structure and function of the human platelet thrombin receptor. Studies using monoclonal antibodies directed against a defined domain within the receptor N terminus. *J Biol Chem* **267:**13795–13798.

Bunemann M, Frank M, and Lohse MJ (2003) G_i protein activation in intact cells involves subunit rearrangement rather than dissociation. *Proc Natl Acad Sci USA* **100:**16077–16082.

Chen CH, Paing MM, and Trejo J (2004) Termination of protease-activated recep-

tor-1 signaling by β-arrestins is independent of receptor phosphorylation. *J Biol Chem* **279:**10020–10031.
Chen J, Ishii M, Wang L, Ishii K, and Coughlin SR (1994) Thrombin receptor activation. Confirmation of the intramolecular tethered liganding hypothesis and discovery of an alternative intermolecular liganding mode. *J Biol Chem* **269:** 16041–16045.
Chung AW, Jurasz P, Hollenberg MD, and Radomski MW (2002) Mechanisms of action of proteinase-activated receptor agonists on human platelets. *Br J Pharmacol* **135:**1123–1132.
Cottrell GS, Coelho AM, and Bunnett NW (2002) Protease-activated receptors: the role of cell-surface proteolysis in signalling. *Essays Biochem* **38:**169–183.
Coughlin SR (1999) How the protease thrombin talks to cells. *Proc Natl Acad Sci USA* **96:**11023–11027.
Coughlin SR (2000) Thrombin signalling and protease-activated receptors. *Nature (Lond)* **407:**258–264.
Debeir T, Benavides J, and Vige X (1996) Dual effects of thrombin and a 14-amino acid peptide agonist of the thrombin receptor on septal cholinergic neurons. *Brain Res* **708:**159–166.
Dowal L, Provitera P, and Scarlata S (2006) Stable association between $G\alpha_q$ and phospholipase Cβ1 in living cells. *J Biol Chem* **281:**23999–24014.
Dupre DJ, Robitaille M, Ethier N, Villeneuve LR, Mamarbachi AM, and Hebert TE (2006) Seven transmembrane receptor core signaling complexes are assembled prior to plasma membrane trafficking. *J Biol Chem* **281:**34561–34573.
Frank M, Thumer L, Lohse MJ, and Bunemann M (2005) G protein activation without subunit dissociation depends on a Gαi-specific region. *J Biol Chem* **280:** 24584–24590.
Galés C, Rebois RV, Hogue M, Trieu P, Breit A, Hébert TE, and Bouvier M (2005) Real-time monitoring of receptor and G-protein interactions in living cells. *Nat Methods* **2:**177–184.
Galés C, Van Durm JJ, Schaak S, Pontier S, Percherancier Y, Audet M, Paris H, and Bouvier M (2006) Probing the activation-promoted structural rearrangements in preassembled receptor-G protein complexes. *Nat Struct Mol Biol* **13:**778–786.
Galvez T, Duthey B, Kniazeff J, Blahos J, Rovelli G, Bettler B, Prezeau L, and Pin JP (2001) Allosteric interactions between GB1 and GB2 subunits are required for optimal $GABA_B$ receptor function. *EMBO (Eur Mol Biol Organ) J* **20:**2152–2159.
Hein P, Frank M, Hoffmann C, Lohse MJ, and Bunemann M (2005) Dynamics of receptor/G protein coupling in living cells. *EMBO (Eur Mol Biol Organ) J* **24:**4106–4114.
Hollenberg MD and Compton JS (2002) International Union of Pharmacology. XXVIII. Proteinase-activated receptors. *Pharmacol Rev* **54:**203–217.
Hynes TR, Mervine SM, Yost EA, Sabo JL, and Berlot CH (2004) Live cell imaging of Gs and the β2-adrenergic receptor demonstrates that both αs and β1γ7 internalize upon stimulation and exhibit similar trafficking patterns that differ from that of the β2-adrenergic receptor. *J Biol Chem* **279:**44101–44112.
Insel PA, Head BP, Patel HH, Roth DM, Bundey RA, and Swaney JS (2005) Compartmentation of G-protein-coupled receptors and their signalling components in lipid rafts and caveolae. *Biochem Soc Trans* **33:**1131–1134.
Janetopoulos C, Jin T, and Devreotes P (2001) Receptor-mediated activation of heterotrimeric G-proteins in living cells. *Science (Wash DC)* **291:**2408–2411.
Kannan S (2002) Role of protease-activated receptors in neutrophil degranulation. *Med Hypotheses* **59:**266–267.
Kusumi A, Nakada C, Ritchie K, Murase K, Suzuki K, Murakoshi H, Kasai RS, Kondo J, and Fujiwara T (2005) Paradigm shift of the plasma membrane concept from the two-dimensional continuum fluid to the partitioned fluid: high-speed single-molecule tracking of membrane molecules. *Annu Rev Biophys Biomol Struct* **34:**351–378.
Lledo PM, Homburger V, Bockaert J, and Vincent JD (1992) Differential G protein-mediated coupling of D2 dopamine receptors to K+ and Ca^{2+} currents in rat anterior pituitary cells. *Neuron* **8:**455–463.
Macfarlane SR, Seatter MJ, Kanke T, Hunter GD, and Plevin R (2001) Proteinase-Activated Receptors. *Pharmacol Rev* **53:**245–282.
Mercier JF, Salahpour A, Angers S, Breit A, and Bouvier M (2002) Quantitative assessment of β1- and β2-adrenergic receptor homo- and heterodimerization by bioluminescence resonance energy transfer. *J Biol Chem* **277:**44925–44931.
Meyer BH, Segura JM, Martinez KL, Hovius R, George N, Johnsson K, and Vogel H (2006) FRET imaging reveals that functional neurokinin-1 receptors are monomeric and reside in membrane microdomains of live cells. *Proc Natl Acad Sci USA* **103:**2138–2143.
Nobles M, Benians A, and Tinker A (2005) Heterotrimeric G proteins precouple with G protein-coupled receptors in living cells. *Proc Natl Acad Sci USA* **102:**18706–18711.
Norton KJ, Scarborough RM, Kutok JL, Escobedo MA, Nannizzi L, and Coller BS (1993) Immunologic analysis of the cloned platelet thrombin receptor activation mechanism: evidence supporting receptor cleavage, release of the N-terminal peptide, and insertion of the tethered ligand into a protected environment. *Blood* **82:**2125–2136.
O'Brien PJ, Prevost N, Molino M, Hollinger MK, Woolkalis MJ, Woulfe DS, and Brass LF (2000) Thrombin responses in human endothelial cells. Contributions from receptors other than PAR1 include the transactivation of PAR2 by thrombin-cleaved PAR1. *J Biol Chem* **275:**13502–13509.
Paing MM, Stutts AB, Kohout TA, Lefkowitz RJ, and Trejo J (2002) beta -Arrestins regulate protease-activated receptor-1 desensitization but not internalization or down-regulation. *J Biol Chem* **277:**1292–1300.
Rebois RV, Robitaille M, Gales C, Dupre DJ, Baragli A, Trieu P, Ethier N, Bouvier M, and Hebert TE (2006) Heterotrimeric G proteins form stable complexes with adenylyl cyclase and Kir3.1 channels in living cells. *J Cell Sci* **119:**2807–2818.
Seeley S, Covic L, Jacques SL, Sudmeier J, Baleja JD, and Kuliopulos A (2003) Structural basis for thrombin activation of a protease-activated receptor: inhibition of intramolecular liganding. *Chem Biol* **10:**1033–1041.
Suzuki K, Ritchie K, Kajikawa E, Fujiwara T, and Kusumi A (2005) Rapid hop diffusion of a G-protein-coupled receptor in the plasma membrane as revealed by single-molecule techniques. *Biophys J* **88:**3659–3680.
Trejo J (2003) Protease-activated receptors: new concepts in regulation of G protein-coupled receptor signaling and trafficking. *J Pharmacol Exp Ther* **307:**437–442.
Vilardaga JP, Bunemann M, Krasel C, Castro M, and Lohse MJ (2003) Measurement of the millisecond activation switch of G protein-coupled receptors in living cells. *Nat Biotechnol* **21:**807–812.
Vu TK, Hung DT, Wheaton VI, and Coughlin SR (1991) Molecular cloning of a functional thrombin receptor reveals a novel proteolytic mechanism of receptor activation. *Cell* **64:**1057–1068.
Yi TM, Kitano H, and Simon MI (2003) A quantitative characterization of the yeast heterotrimeric G protein cycle. *Proc Natl Acad Sci USA* **100:**10764–10769.

Address correspondence to: Dr. Jean-Philippe Pin, Institut de Génomique Fonctionnelle; Département de Pharmacologie Moléculaire; 141, rue de la Cardonille, Montpellier F-34094 Cedex 5, France. E-mail: jppin@igf.cnrs.fr